Basal Cell Carcinoma

13

Manuj Agarwal and Ajay Bhatnagar

Contents

13.1 Epidemiology

Non-melanoma skin cancers (NMSC) are the most commonly diagnosed malignant neoplasms in the Caucasian population of the United States. Eighty percent of cases are basal cell carcinomas (BCC), but a reliable estimate of incidence is imprecise

M. Agarwal (✉)
Department of Radiation Oncology, Penn Presbyterian Medical Center, Philadelphia, PA, USA

A. Bhatnagar
Prostate Cancer Institute of Arizona, Casa Grande, AZ, USA
e-mail: drajay@pciaz.org

E. Kim et al. (eds.), *Radiation Therapy for Sarcomas and Skin Cancers*, Practical Guides in Radiation Oncology, https://doi.org/10.1007/978-3-031-06706-8_13

due to lack of registration in cancer registries [1]. The National Cancer Institute estimates that approximately 5.4 million NMSC cases were diagnosed in 2012, and the majority were BCC [2]. Fair-skinned individuals are more commonly affected, and the incidence of BCC in white patients has risen more than 10% per year with resultant increase in associated treatment procedures and healthcare expense [3, 4].

13.2 Natural History

BCC arises from the basal layer of epidermis and its appendages. It commonly develops from hair follicles. Approximately 70% arise on the sun-exposed head and neck and 15% present on the trunk. While it is considered an indolent process, BCC can be locally invasive resulting in disfigurement and may result in destruction of surrounding structures. The particular biological behavior may vary by histologic subtype (see below).

Tumors have a low propensity for nodal or distant metastases with an overall incidence of 0.01% [5]. When spread does occur, it does so in a stepwise fashion, progressing first in regional nodes and then distantly. Spread is usually associated with locally advanced disease. Perineural/neurotropic involvement is rare, occurring in only 2% of cases and is associated with aggressive histology [5].

While BCC is associated with low mortality, it can result in decreased quality of life and significant healthcare costs.

13.3 Subtypes

BCC lesions may present in a variety of manifestations, depending on the lesion histopathology. Each has its distinctive clinical and histologic features and may have a varying natural history [6–9].

Subtype	Incidence	Location	Appearance	Presentation
Nodular (Fig. 13.1)	80%	H&N	Color: pink/flesh-colored. Pearly/translucent. May have varying degree of pigment Shape: papule Other features: – Telangiectasia. – "Rolled" border"– Periphery is more raised than the middle – Ulceration frequent	Slow growth. May result in peripheral and deep invasion and perineural spread

Subtype	Incidence	Location	Appearance	Presentation
Superficial (Fig. 13.2)	15%	Trunk	Color: light red to pink. May have spotty brown/ black pigment Shape: macules, patches or thin plaques Other: – Slightly scaly – Non-firm – Center may be atrophic – Periphery may be indistinct and rimmed with fine translucent papules	Slow, superficial progression. May become nodular or ulcerative over years
Morpheaform/ sclerosing (Fig. 13.3)	5%	H&N	Color: pink/flesh-colored Shape: papules or plaques Other – Flat, firm, or indurated – Frequently atrophic – Ill-defined borders	Aggressive growth. May result in peripheral or deep invasion. Perineural invasion more common.
Infiltrative (Fig. 13.4)	<5%	H&N	Color: Opaque or yellow Other – Blends subtly with the surrounding skin	Aggressive growth. May result in peripheral or deep invasion

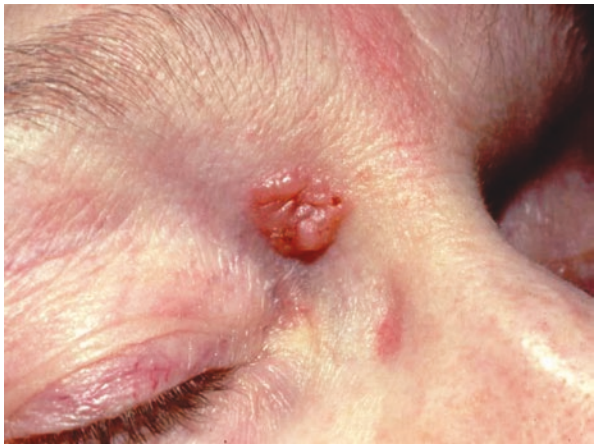

Fig. 13.1 Nodular basal cell carcinoma. Image reproduced with permission from Michael L Ramsey, MD, Geisinger Medical Center, published by Medscape Drugs & Diseases (https://emedicine.medscape.com/), Basal Cell Carcinoma, 2019, available at: https://emedicine.medscape.com/article/276624-overview

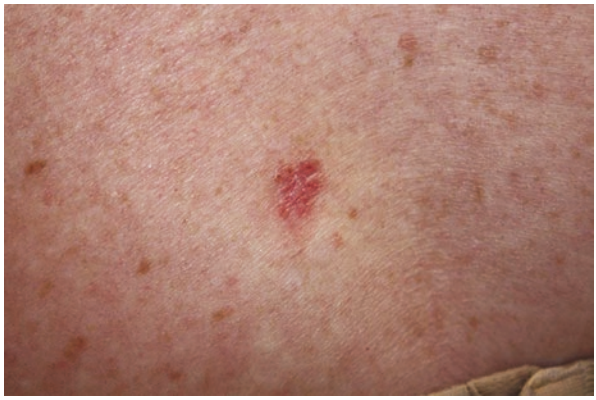

Fig. 13.2 Superficial basal cell carcinoma. Image reproduced with permission from Robert S Bader, MD, Broward Health, published by Medscape Drugs & Diseases (https://emedicine.medscape.com/), Basal Cell Carcinoma, 2019, available at: https://emedicine.medscape.com/article/276624-overview

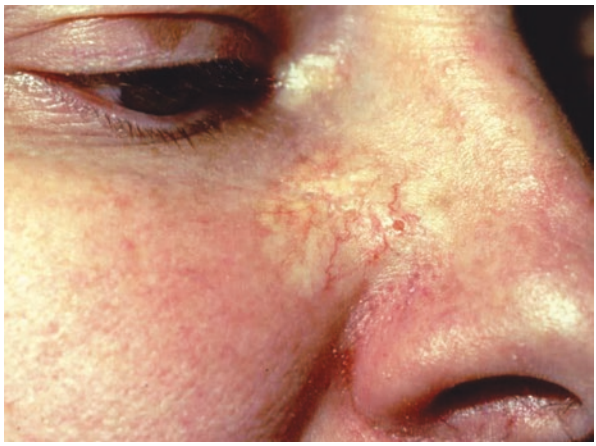

Fig. 13.3 Morpheaform basal cell carcinoma: image reproduced with permission from Michael L Ramsey, MD, Geisinger Medical Center, published by Medscape Drugs & Diseases (https://emedicine.medscape.com/), Basal Cell Carcinoma, 2019, available at: https://emedicine.medscape.com/article/276624-overview

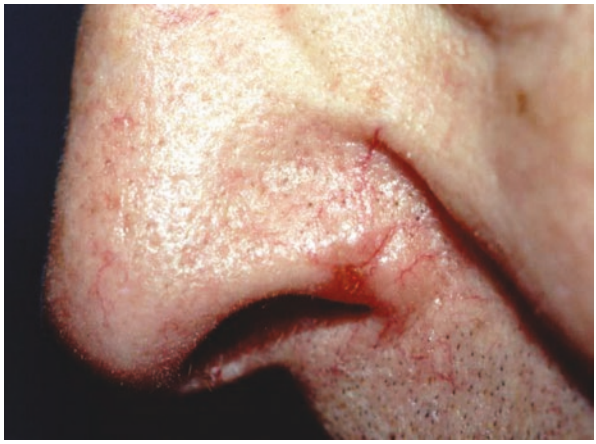

Fig. 13.4 Infiltrative basal cell carcinoma: image reproduced with permission from Michael L Ramsey, MD, Geisinger Medical Center, published by Medscape Drugs & Diseases (https://emedicine.medscape.com/), Basal Cell Carcinoma, 2019, available at: https://emedicine.medscape.com/article/276624-overview

Other, rare BCC subtypes have been described including basosquamous cell carcinoma that may behave aggressively.

13.3.1 Risk Stratification

Cutaneous carcinomas of the H&N, including BCCs of the region, are staged according to the eighth edition of the AJCC Cancer Staging Manual (Table 13.1) [10]. Exceptions include carcinomas of the eyelid and Merkel cell carcinomas. There is no staging system for cutaneous carcinomas outside of the H&N region.

The majority of BCC lesions present early and treatment is based rather on risk factors for recurrence rather than stage. NCCN guidelines has defined criteria for "low risk" and "high risk" of recurrence (Table 13.2) [11]. Note that the presence of any high-risk factor places the patient in the high-risk category.

Table 13.1 Staging BCC of the H&N

Primary tumor (T)	
T category	T criteria
TX	Primary tumor cannot be assessed
Tis	Carcinoma in situ
T1	Tumor smaller than or equal to 2 cm in greatest dimension
T2	Tumor larger than 2 cm but smaller than or equal to 4 cm in greatest dimension
T3	Tumor larger than 4 cm in maximum dimension or minor bone erosion or perineural invasion or deep invasion[a]
T4	Tumor with gross cortical bone/marrow, skull-base invasion and/or skull-base foramen invasion
T4a	Tumor with gross cortical bone/marrow invasion
T4b	Tumor with skull-base invasion and/or skull-base foramen involvement
Regional lymph nodes (N)	
Clinical N (cN)	
N category	**N criteria**
NX	Regional lymph nodes cannot be assessed
N0	No regional lymph node metastasis
N1	Metastasis in a single ipsilateral lymph node, 3 cm or smaller in greatest dimension and ENE(−)
N2	Metastasis in a single ipsilateral node larger than 3 cm but not larger than 6 cm in greatest dimension and ENE(−) Metastases in multiple ipsilateral lymph nodes, none larger than 6 cm in greatest dimension and ENE(−) In bilateral or contralateral lymph nodes, none larger than 6 cm in greatest dimension and ENE(−)
N2a	Metastasis in a single ipsilateral node larger than 3 cm but not larger than 6 cm in greatest dimension and ENE(−)
N2b	Metastases in multiple ipsilateral lymph nodes, none larger than 6 cm in greatest dimension and ENE(−)

(continued)

Table 13.1 (continued)

Primary tumor (T)	
T category	T criteria
N2c	Metastases in bilateral or contralateral lymph nodes, none larger than 6 cm in greatest dimension and ENE(−)
N3	Metastasis in a lymph node larger than 6 cm in greatest dimension and ENE(−) Metastasis in any node(s) and clinically overt ENE [ENE(+)]
N3a	Metastasis in a lymph node larger than 6 cm in greatest dimension and ENE(−)
N3b	Metastasis in any node(s) and ENE(+)
Note*:* A designation of "U" or "L" may be used for any N category to indicate metastasis above the lower border of the cricoid (U) or below the lower border of the cricoid (L). Similarly, clinical and pathological ENE should be recorded as ENE(−) or ENE(+)	
Pathological N (pN)	
N category	**N criteria**
NX	Regional lymph nodes cannot be assessed
N0	No regional lymph node metastasis
N1	Metastasis in a single ipsilateral lymph node, 3 cm or smaller in greatest dimension and ENE(−)
N2	Metastasis in a single ipsilateral lymph node, 3 cm or smaller in greatest dimension and ENE(+) Larger than 3 cm but not larger than 6 cm in greatest dimension and ENE(−) Metastases in multiple ipsilateral lymph nodes, none larger than 6 cm in greatest dimension and ENE(−) In bilateral or contralateral lymph node(s), none larger than 6 cm in greatest dimension, ENE(−)
N2a	Metastasis in a single ipsilateral lymph node, 3 cm or smaller in greatest dimension and ENE(+) A single ipsilateral lymph node larger than 3 cm but not larger than 6 cm in greatest dimension and ENE(−)
N2b	Metastases in multiple ipsilateral lymph nodes, none larger than 6 cm in greatest dimension and ENE(−)
N2c	Metastasis in bilateral or contralateral lymph node(s), none larger than 6 cm in greatest dimension and ENE(−)
N3a	Metastasis in a lymph node larger than 6 cm in greatest dimension and ENE(−)
N3b	Metastasis in a single ipsilateral node larger than 3 cm in greatest dimension and ENE(+) Multiple ipsilateral, contralateral, or bilateral nodes, any with ENE(+) A single contralateral node of any size and ENE(+)
Note*:* A designation of "U" or "L" may be used for any N category to indicate metastasis above the lower border of the cricoid (U) or below the lower border of the cricoid (L). Similarly, clinical and pathological ENE should be recorded as ENE(−) or ENE(+)	

Table 13.1 (continued)

Primary tumor (T)			
T category	T criteria		
Distant metastasis (M)			
M category	**M criteria**		
M0	No distant metastasis		
M1	Distant metastasis		
Prognostic stage groups			
When T is...	**And N is...**	**And M is...**	**Then the stage group is...**
Tis	N0	M0	0
T1	N0	M0	I
T2	N0	M0	II
T3	N0	M0	III
T1	N1	M0	III
T2	N1	M0	III
T3	N1	M0	III
T1	N2	M0	IV
T2	N2	M0	IV
T3	N2	M0	IV
Any T	N3	M0	IV
T4	Any N	M0	IV
Any T	Any N	M1	IV

[a]Deep invasion is defined as invasion beyond the subcutaneous fat or >6 mm (as measured from the granular layer of adjacent normal epidermis to the base of the tumor); perineural invasion for T3 classification is defined as tumor cells within the nerve sheath of a nerve lying deeper than the dermis or measuring 0.1 mm or larger in caliber or presenting with clinical or radiographic involvement of named nerves without skull-base invasion or transgression

Table 13.2 Risk factors for recurrence

	Low risk	High risk
Location/size	Area $L < 20$ mm Area $M < 10$ mm	Area $L \geq 20$ mm Area $M \geq 10$ mm Area H
Borders	Well defined	Poorly defined
Primary vs recurrent	Primary	Recurrent
Immunosuppression	No	Yes
Site of prior RT	No	Yes
Pathologic subtype	Nodular Superficial	Aggressive growth pattern
Perineural involvement	Negative	Positive

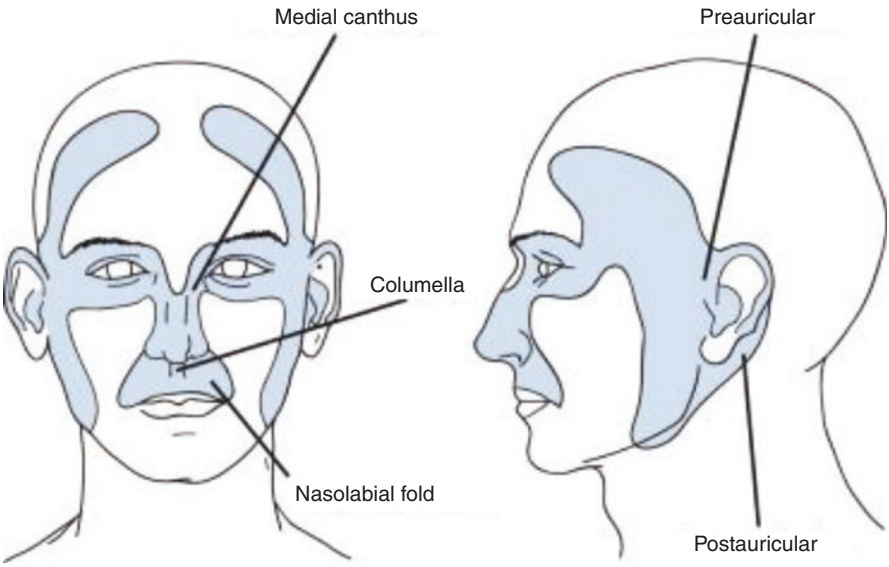

Fig. 13.5 *H* zone of the face. Reprinted from Clinical Radiation Oncology fourth Edition, M. Veness and J. Howle, Cutaneous Carcinoma, 2016, with permission from Elsevier

Figure 13.5 depicts the *M* and *H* zones of the face. Area *L* includes the trunk and extremities but excludes with hands, nail units, pretibial skin, ankles, and feet. The *H* zone is located at the midface and includes the periauricular region, glabella, medial canthus, nose, nasolabial region, and columella [11]. The region contains embryonal fusion planes, and histopathology often reveals extensive infiltration of deeper structures. Due to its location, there is understandable high concern for optimal cosmetic and functional outcome, which drives the employment of narrow surgical and radiation margins. Thus, lesions involving the *H* zone are at high risk for recurrence regardless of size. Tissue-sparing techniques, such as MOHS and staged excision, are recommended in order to have complete complex margin assessment.

13.3.2 Management Options

13.3.2.1 Excision

Standard excision with postoperative margin assessment has been employed for decades and results in a 5-year local control of approximately 98% [12]. For low-risk lesions, a 4 mm margin will result in complete removal in over 95% of cases [13]. A wider margin is recommended for high-risk lesions. If tissue rearrangement or a skin graft is required to close the surgical defect, intraoperative margin assessment is recommended before closure.

13.3.2.2 MOHS Micrographic Surgery (MMS)

MMS is the preferred surgical technique for high-risk lesions as it allows for intraoperative margin assessment. When compared to standard excision, MMS is associated with improved local control in both the primary and locally recurrent setting, 1% vs 10.1% and 5.6% vs 17.4%, respectively [14].

13.3.2.3 Curettage and Electrodesiccation (C&E)

C&E involves scraping away of a tumor with a curette and denaturing the area with electrodesiccation. It does not allow for margin assessment. While some reports demonstrate a 5-year local control ranging from 91 to 97%, others note 20–30% recurrence rates [12].

13.3.2.4 Superficial Therapies

Topical therapies, cryosurgery, and photodynamic therapy result in inferior local control and should be reserved for patients who cannot undergo surgery or radiation therapy. The five-year local control is in the 80% range [15].

13.3.3 Radiation Therapy

13.3.3.1 Patient Selection

Patient referred for radiotherapy are typically older and may have contraindications to surgery due to competing comorbidities or advanced age. The five-year local control ranges from 92 to 96% for external beam and 95 to 99% for brachytherapy [16, 17]. It is important to note that these figures are laden with bias, as patients who are referred may have tumors in less optimal areas, where expansion margins are compromised.

13.3.3.2 Modality Comparison

To date, there is only one report of level one evidence comparing surgery or radiotherapy. This trial compared 347 patients treated from 1982 to 1987 at Goustave-Roussy and reported a 4-year local control rate of 0.7% for surgery and 7.5% for radiation as well as patient reported "good" cosmesis of 87 vs 69%. It is important to note that radiation in this trial was not standard and is quite outdated. Fifty-five percent of patients received LDR interstitial therapy and 33% received superficial contact therapy [18]. The relevance of this data to modern radiation therapy is limited.

More recently, a systematic review identified key observational studies that assessed tumor recurrence after a variety of treatment modalities (Table 13.3) [17].

Brachytherapy was recently compared to MMS in a matched pair analysis [19]. At a median follow-up of 3.5 years, local control was 99.5% for brachytherapy and 100% for MMS ($p = 1.00$) in 208 lesions each, respectively. There was no difference in patient reported or clinician reported cosmesis.

Table 13.3 Modality comparison

Modality	LR	CI	# Prospective reports
Excision	5.4%	2.5–9.1	12
MOHS	3.0%	2.2%–3.9%	10
EBRT	6.4%	3.0%–11.0%	7
Brachy	5.2%	1.6–10.5%	4

13.3.3.3 Treatment Recommendations

Low-risk lesions include C&E in areas without hair growth, standard excision with postoperative margin assessment, or radiation therapy. High-risk lesions may be treated with MMS, standard excision with postoperative margin assessment, or radiation therapy [11]. Postoperative radiation is recommended for high-risk patients with close/positive margins, extensive PNI, or named nerve involvement.

13.3.4 Radiation Techniques

A variety of techniques may be utilized to treat BCC. This depends on the tumor location, size, and depth. Prescription dose and fractionation may vary based on these factors, as well as desired cosmesis and functional consideration.

13.3.5 External Beam Radiation

13.3.5.1 Orthovoltage/Supervoltage

Superficial x-ray (usually 75–300 kVp) units such as these deposit a maximum dose (*D*max) at the skin surface with exponential decrease in dose with depth. These units are no longer widely available.

13.3.5.2 Electron Beam

Modern linear accelerators produce electron energies from 6 to 20 MeV, offering varying degrees of dose fall off depending on the depth of treatment desired. Low-dose, 6–9 MeV energies are most commonly utilized. Electrons offer a region of uniform dose followed by rapid dose falloff.

Depth-dose profiles for commonly used energies can be obtained from beam data detailing depth-dose profiles specific to their linear accelerator. Differences between linear accelerators can be clinically significant.

The electron beam energy chosen reflects the depth of tissue requiring treatment. Electrons are moderately "skin sparing," particularly at low energies due to scatter, with *D*max below skin surface. As a result, placement of a tissue equivalent material (bolus) on the skin is commonly used to draw the beam isodose lines to the skin surface (Fig. 13.6). A flexible bolus is preferred to better conform to the skin surface.

The thickness of bolus considered depends on the energy chosen with a goal of placing Dmax at the skin surface and the 90% isodose line including bolus a few

Fig. 13.6 Superflab bolus. Courtesy of Civco Radiotherapy

millimeters deeper than the base of the lesion [20]. A commonly used estimate for the depth in cm at which the 90% isodose line will be is the electron energy divided by 4. For example, a 12 MeV electron energy likely will be effective to a 3 cm depth. The depth-dose curve falls sharply thereafter. When in doubt, it is recommended to use a higher energy to ensure coverage of the target [21].

Electron beam therapy is prescribed "en face," a French term for facing forward. The gantry of the linac must be rotated so that the beam axis is perpendicular to the surface to be treated. Electrons are best employed on flat skin surfaces. The depth-dose profiles, above, are measured in a water bath. Beam perturbation increased with obliquity and greatly affects dose profile. Obliquity results in increased side scatter, a shift in Dmax to the surface, and decreased depth of penetration. Uneven air gaps and sharp surface irregularities produce localized hot and cold spots [21]. For lesions with sharp angles and irregularity, such as the nose, ear, periorbital region, and extremities, brachytherapy may be preferable (see below).

Patient-specific, custom bolus may be utilized and may be preferred in regions with large irregularities and obliquities. These devices may be uniform or, more commonly, variable thickness. A number of "in-house" or industry solutions may be utilized. Bolus may be handmade using thermoplastic sheets, thermoplastic pellets, or dental putty. These methods may be error prone due to inconsistent thickness during the molding process, may result in undesired air gaps, and may have limited durability. Air gaps may result in scattering of electrons and reduction in dose.

A modern solution that has been introduced in many institutions utilizes 3D printers. Institution-specific or commercially available software is available that can create a bolus from DICOM data transmitted from the patient's CT data set. Tissue-equivalent filament material is utilized. Commercially available custom bolus includes BolusECT from dotdecimal and Modulated Electron Bolus from both Civco and Adaptiiv. Figure 13.7 illustrates the advantage of using a 3D bolus, while Fig. 13.8 depicts an example of 3D-printed bolus.

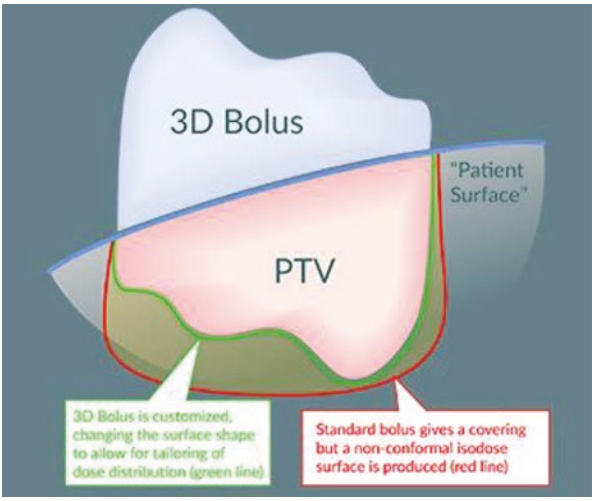

Fig. 13.7 3D bolus cartoon. Courtesy of Adaptiiv

Fig. 13.8 Example of 3D-printed bolus. Courtesy of Adaptiiv

13.3.5.3 Patient Setup

For small, early-stage lesions, simulation may be largely clinical, and CT simulation may not be required. Larger, irregular, bulky lesions or lesions in regions with minimal subcutaneous tissue, such as a periorbital lesion, may benefit from CT simulation to better delineate tumor thickness.

On the treatment table, the patient should be immobilized in a reproducible position. It is preferable that the plane of the skin to be treated is horizontal and perpendicular to the linac gantry. Horizontal positioning may facilitate the placement of bolus and lead shield for skin collimation, if utilized.

The lesion is visualized and a margin drawn on the patient with a marker with assistance of a ruler. Once finalized, if the patient is to undergo CT, this margin is then "wired" using radiopaque linear markers that can be visualized by CT. Surgical literature suggests a 4 mm GTV to CTV expansion for low-risk lesions and 6 mm for high-risk lesions [13]. Note that infiltrative lesions may have greater subclinical

disease extension and would require a more generous margin. The additional margin from CTV to PTV depends on the field size and energy to be utilized, as well as whether beam collimation will take place at the cone or on the patient's skin.

Skin to surface distance (SSD) is typically 100 cm, while the measured distance will be less, depending on the thickness of bolus utilized. An electron cone is fitted to the linac treatment head. This applicator is available in several sizes and serves to collimation the electrons to attenuate lateral scatter. The cone is positioned a few cm from the desired treatment surface. The distal part of the cone is fitted with an aperture, which can facilitate the placement of an electron cutout for collimation.

The most widely used method is collimation at the cone. The lead cutout is most commonly constructed using Lipowitz metal (trade name Cerrobend). This metal is an alloy that can be shaped at relatively low temperatures. Most institutions construct the cutout in a designated, on-site, mold room. There are commercial solutions available that can obviate the mold room, such as dotdecimal electron cutout [22]. The minimum thickness of lead required for blocking a given electron energy to <5% transmission is energy divided by 2. An additional mm may be added for safety. The thickness required for Cerrobend is 20% greater than that of lead [21].

When collimating at the cone, the treatment field typically encompasses tumor plus a 1.5–2 cm margin. Margins may be reduced when treating tumors close to a critical structure such as the eye. It should be noted that reduced margins have been associated with reduced local control from electron beam therapy. One may consider skin collimation in this case, or use an alternative modality, such as excision or brachytherapy.

Caution should be exercised when treating with a small field size. Central axis depth dose is field size dependent, with dose decreasing with decreasing field size due to decreased scatter. Depth dose may be reduced for small field sizes or extensive blocking with Dmax shifting to the surface, compared to broad beams. It is recommended that the overall size of the cutout should be large enough so that the cone/collimator setting is at least 4 × 4 cm [21].

Skin collimation may also be employed when using low energy electrons (Fig. 13.9). Skin collimation is not employed for higher energy electrons, as thicker lead is required which is not as easily molded and may result in patient discomfort. This technique places a 3–4 mm thick lead cutout directly on the skin surface. Due to its thin nature, the lead sheets may be molded to conform to the surface contour. It is used for field shaping and conforms to the geometry of the desired volume. As collimation is taking place on the skin rather than scattering in air, expansion margins may be reduced [21, 23].

Special shielding devices are recommended when treating lesions near the eye, nose, mouth, and ear. For the eye, after topical anesthetic placement, a tungsten shield is placed directly under the eyelids to protect the lens and superficial eye structures. This eye shield reduces the dose to <5% for energies up to 9 MeV (Fig. 13.10).

"Exit dose" blocking is employed for lesions of the other aforementioned sites using internal shielding (Fig. 13.11). The nasal septum, nasal canal, and underlip/gingival/buccal regions of the oral cavity are shielded with lead strips coated with

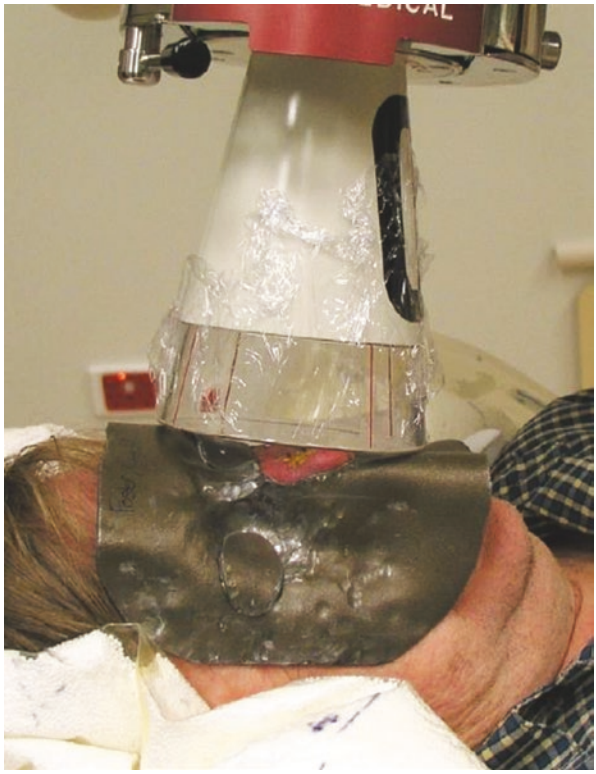

Fig. 13.9 Example of skin collimation. Patient undergoing electron beam therapy to the left nose. Note additional layer of lead over eyes to further reduce scattered dose. Reprinted from Clinical Radiation Oncology fourth Edition, M. Veness and J. Howle, Cutaneous Carcinoma, 2016, with permission from Elsevier

Fig. 13.10 Tungsten eye shields. Courtesy of Civco Radiotherapy

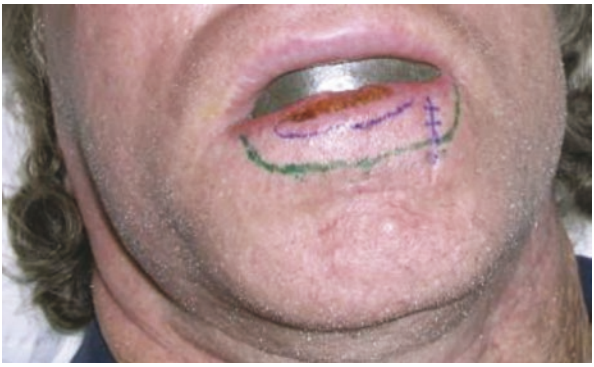

Fig. 13.11 Example of an oral cavity lead shield. This patient is receiving definitive radiotherapy for a lower lip carcinoma. Reprinted from Clinical Radiation Oncology 4th Edition, M. Veness and J. Howle, Cutaneous Carcinoma, 2016, with permission from Elsevier

wax or acrylic. The coating serves to absorb electron backscatter from the lead, which can be quite substantial [24].

Given the numerous variables noted above, as well as a degree of discrepancy between dose computed on a treatment planning system compared to actual dose measured on a patient, it is recommended that in vivo dosimetry be performed. There are a number of methods for remote determination of absorbed dose using in vivo dosimetry. These methods include thermoluminescent dosimeters (TLD) and optically stimulated luminescent dosimeter (OSLD). The readout process for OSLDs is more time efficient and thus more commonly employed.

If there is a clinically relevant discrepancy between calculated dose and measured dose, one may use the measurement to calculate dose scaling.

13.3.5.4 Prescription

Several fractionation schedules may be utilized in the treatment of BCC with EBRT. The dose for irradiation with electrons is prescribed at 90%. In general, more protracted schedules using lower dose (2–2.5 Gy) per fraction achieves the most optimal cosmetic results. Other factors that are considered include age, lesion size, and site. For most patients, 50–55 Gy in 20 fractions is effective with acceptable cosmesis and low toxicity. A more hypofractionated approach of 40 Gy in 10 fractions of 30 Gy in 5 fractions may be employed for a patient with poor performance status or limited transportation ability. A dose shorter than 4 weeks is not recommended in the adjuvant setting [11]. When treating lesions near a critical organ, such as the eye, it is important to consider organ tolerance. Dose constraints are provided in 2 Gy/fx, and if an alternative prescription is used, EQD2 calculations may be necessary.

13.3.5.5 Electron Arc Therapy

Arc therapy is commonly employed with photons to deliver IMRT treatments. It may also be employed in electron beam delivery to treat superficial tumors along curved surfaces. Instances in which this technique would be useful include large limb lesions as well as chest wall lesions that extend across the midaxillary line and anterior/posteriorly. Electron arcs may prove to be superior to abutting electron

fields to prevent field junction problems and superior to photons to avoid unnecessary irradiation of underlying tissue. Many linacs are either not equipped or not commissioned for electron arc therapy, and its clinical use is limited [21].

13.3.5.6 Photon Beam Therapy

Photons are rarely employed in the treatment of BCC. Extensive, deeply infiltrating tumors, especially those with bone or cartilage involvement, may require mixed electron-photon therapy, or photon therapy alone.

13.3.5.7 Brachytherapy

Skin brachytherapy (BT) may be delivered via superficial applicators or interstitial techniques. Superficial BT, as the name implies, is delivered to skin surface lesions. Interstitial BT utilizes rigid needles or plastic tubes and is applied to deeper, bulkier lesions. Surface BT may be delivered using low-dose rate (LDR), pulsed dose rate (PDR), high-dose rate (HDR), or electronic. Interstitial BT may be similarly delivered with the exception of electronic. In clinical practice, HDR and electronic BT are most commonly utilized.

There are several potential advantages of BT over EBRT. Prescriptions are hypofractionated, typically 6–10 in total, offering patient convenience. Dose is delivered in a short time, typically in the order of minutes. Most notably, dose from a brachytherapy source follows the inverse square law, allowing for optimal dose distribution to a tumor with rapid dose fall off. This may translate to less dose to surrounding normal tissue [25, 26].

13.3.6 Applicators

13.3.6.1 Contact BT

Small lesions on regular surfaces may be treated by shielded superficial radionuclide applicators. Two commercially applicators are available, namely, the Leipzig (Elekta and Varian) and Valencia (Elekta) applicators. The Leipzig applicator is cup shaped, composed of tungsten, and available in a range of diameters. The HDR source emerges as its vertex and results in non-flat dose distribution, resulting in an inhomogeneous dose to the target. The Valencia applicator adds a flattening filter to homogenize dose distribution. This added attenuation results increased treatment time. With a typically treatment depth of 3 mm, the skin surface dose is approximately 135%. A 1 mm plastic cover cap remains on the Valencia applicator and serves to maintain this low surface dose. Removal may increase surface dose by a factor of 2.8.

A transparent acrylic template, La Fe-ITIC, may be utilized to assist with delineating appropriate expansions and applicator selection [27].

13.3.6.2 Surface Flaps

Commercially available flaps may be utilized for larger surfaces without significant irregularity. Examples include the chest wall, cheek, and dorsum of the hand and foot. These consist of a single layer of silicone rubber material 10 mm in diameter with

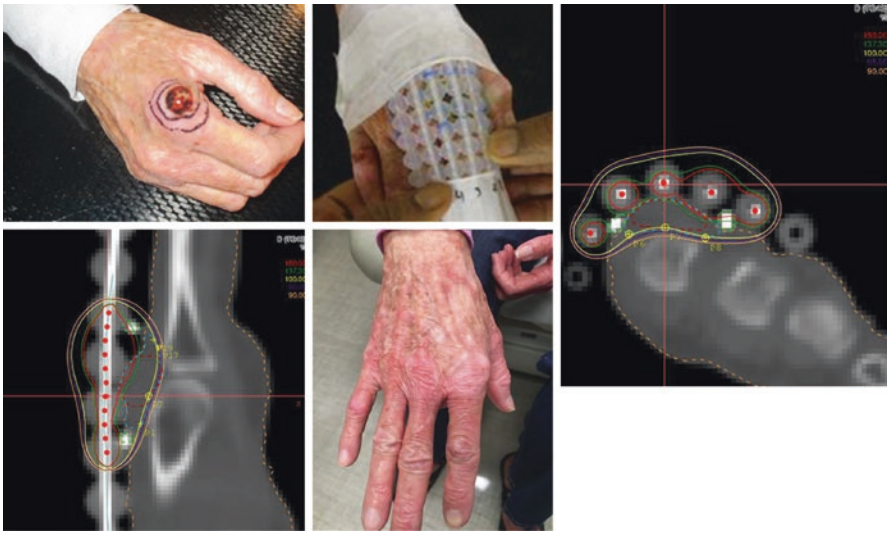

Fig. 13.12 Case example of a 41-year-old woman on immunosuppression for autoimmune hepatitis who developed lesion over the right second metacarpophalangeal joint treated with surface brachytherapy using a Frieberg flap

catheters embedded through the center. This ensures a 5 mm source to skin distance. Available flaps include the Freiburg™ flap (Elekta Instrument AB, Stockholm, Sweden), the H.A.M.™ (Mick Radio-Nuclear Instruments and Eckert & Ziegler BEBIG, Berlin, Germany), and the Catheter Flap set™ (Varian Medical Systems, Palo Alto, CA, USA). Figure 13.12 demonstrates a case example of a Freiburg flap.

13.3.6.3 Custom Applicators

Custom surface mounds may be created for irregular surfaces, such as the nose, fingers, and pinna. Similar to the custom bolus described above, these may be constructed using polymers, acrylic resin, dental wax, or a thermoplastic material. Molds are adapted to the patient surface, and catheters are embedded/weaved through. A common application includes the use of a thermoplastic mask with catheters adherent to wax or resin.

3D-printed custom applicators may be fabricated with customized catheter positions that follow the patient's anatomy (Fig. 13.13). Similar to 3D-printed electron bolus, the patient's DICOM data from their CT simulation is digitized.

13.3.6.4 Treatment Planning and Prescription

Surface brachytherapy is typically prescribed to a depth of 3–5 mm. Tumors greater than 5 mm cannot be adequately treated to depth without substantial skin dose. In these cases, interstitial BT or EBRT should be considered.

Brachytherapy is typically delivered every other day. Commonly used prescriptions include 42 Gy in 6 fractions, 40 Gy in 8 fractions, or 40 Gy in 10 fractions. A more protracted fractionated may be employed for larger targets as well as for the pretibial location [27, 28].

Fig. 13.13 3D-printed custom applicator for a nose case. Courtesy of Adaptiiv

13.3.6.5 Treatment Toxicity and Patient Management

Treatment of a skin cancer with radiation will result in moist desquamation toward the end of treatment or shortly thereafter depending on the fractionation employed. Typical precautions include avoidance of heat, cold, sunlight, friction, and harsh skin products. During treatment, daily moisturization with a bland emollient is recommended. Moist desquamation is managed with the application of silver sulfadiazine cream. Following recovery, patients are instructed to exercise lifetime sun precautions over the irradiated area. Late effects may include hypopigmentation, hyperpigmentation, telangiectasis, fibrosis, and skin atrophy. It is recommended that patients follow routinely with dermatology as they are at high risk for developing an additional primary cutaneous malignancy over their sun-damaged skin.

13.3.6.6 Palliation

Patients with neglected BCC may present with locally advanced disease involving bone, cartilage, muscle, or nerves. They may not be amenable to definitive intent therapy and may be effectively palliated with radiation. Radiation may reduce local morbidity, such as pain and bleeding. Optimal dose fractionation depends on tumor bulk, location, and the patient's life expectancy.

13.4 Systemic Therapy

Systemic therapy for BCC is not often employed and reserved for patients with locally advanced disease not amenable to definitive or palliative local therapy and patients with numerous lesions (often associated with immunosuppression or genetic predisposition) or the rare instance of distant metastases.

13.4.1 Targeted Therapy: Hedgehog Pathway

Aberrant signaling of the hedgehog (Hh) pathway is a pivotal defect in the pathogenesis of BCC [29]. Signaling is initiated by the cell surface receptor smoothened homolog (SMO). SMO is normally is inhibited by another cell surface receptor, the patched homolog 1 (PTCH1). Hedgehog ligand binding to PTCH1 prevents this

inhibition and facilitates cell proliferation. Mutations of PTCH1 or SMO may result in constitutive pathway activation [30].

Vismodegib and sonidegib are SMO inhibitors that have phase II data supporting its use [31, 32]. A meta-analysis of studies evaluating the two agents noted a similar overall objective response rate 62 and 55%, respectively, for locally advanced disease. In patients with metastatic disease, the response rates were 39 and 15%, respectively. In the setting of limited data, either agent is appropriate [33].

13.4.2 Non-Targeted Agents

Itraconazole is an antifungal agent that inhibits the hedgehog signaling pathway, but data supporting its use is limited data [34].

Chemotherapy. Small case series suggest response with platinum-containing regimens [35].

References

1. Verkouteren JAC, Ramdas KHR, Wakkee M, Nijsten T. Epidemiology of basal cell carcinoma: scholarly review. Br J Dermatol. 2017;177(2):359–72. https://doi.org/10.1111/bjd.15321. Epub 2017 Feb 20.
2. American Cancer Society. Cancer Facts & Figures 2019. Atlanta: American Cancer Society; 2019.
3. Rogers HW, et al. Incidence estimate of nonmelanoma skin Cancer in the United States. Arch Dermatol. 2010;146(3):283–7.
4. Chen et al. The economics of skin Cancer: an analysis of medicare payment data. PRS Global Open 2016 1–7.
5. Geist DE, Garcia-Molner M, Fitzek MM, et al. Perineural invasion of cutaneous squamous cell carcinoma and basal cell carcinoma: raising awareness and optimizing management. Dermatol Surg. 2008;34:1642–51.
6. Rubin AI, Chen EH, Ratner D. Basal cell carcinoma. N Engl J Med. 2005;353:2262–9.
7. Marcil I, Stern R. Risk of developing a subsequent non-melanoma skin cancer. J Am Acad Dermatol. 1990;23:1114–8.
8. Scrivener Y, Grosshans E, Cribier B. Variations of basal cell carcinomas according to gender, age, location and histopathological subtype. Br J Dermatol. 2002;147(1):41.
9. Szewczyk M, Pazdrowski J, Danczak-Pazdrowska A, Golusinski P, Majchrzak E, Luczewski L, Marszałek S, Silny W, Golusinski W. Analysis of selected recurrence risk factors after treatment of head and neck basal cell carcinoma. Postępy dermatologii i alergologii. 2014;31:146–51. https://doi.org/10.5114/pdia.2014.40959.
10. Califano JA, Lydiatt WM, Nehal KS, et al. Cutaneous squamous cell carcinoma of the head and neck. In: Amin MB, editor. AJCC Cancer Staging Manual. 8th ed. New York: Springer; 2017. p. 171.
11. National Comprehensive Cancer Network. Basal Cell Skin Cancer Version 1.2019. https://www.nccn.org/professionals/physician_gls/pdf/nmsc.pdf. Accessed 7 Aug 2019.
12. Rowe DE, Carroll RJ, Day CL Jr. Long-term recurrence rates in previously untreated (primary) basal cell carcinoma: implications for patient follow-up. J Dermatol Surg Oncol. 1989;15(3):315–28.
13. Wolf DJ, Zitelli JA. Surgical margins for basal cell carcinoma. Arch Dermatol. 1987;123(3):340–4.

14. Rowe DE, Carroll RJ, Day CL Jr. Mohs surgery is the treatment of choice for recurrent (previously treated) basal cell carcinoma. J Dermatol Surg Oncol. 1989;15(4):424–31.
15. Roozeboom MH, Arits AH, Nelemans PJ, Kelleners-Smeets NW. Overall treatment success after treatment of primary superficial basal cell carcinoma: a systematic review and meta-analysis of randomized and nonrandomized trials. Br J Dermatol. 2012;167(4):733–56. https://doi.org/10.1111/j.1365-2133.2012.11061.x. Epub 2012 Sep 7.
16. Wilder RB, Kittelson JM, Shimm DS. Basal cell carcinoma treated with radiation therapy. Cancer. 1991;68(10):2134–7.
17. Lansbury L, Bath-Hextall F, Perkins W, Stanton W, Leonardi-Bee J. Interventions of non-metastatic squamous cell carcinoma of the skin: systemic review and pooled analysis of observational studies. BMJ. 2013;347:f6153. https://doi.org/10.1136/bmj.f6153.
18. Avril MF, Auperin A, Margulis A, Gerbaulet A, Duvillard P, Benhamou E, Guillaume JC, Chalon R, Petit JY, Sancho-Garnier H, Prade M, Bouzy J, Chassagne D. Basal cell carcinoma of the face: surgery or radiotherapy? Results of a randomized study. Br J Cancer. 1997;76(1):100–6.
19. Patel R, et al. Comparison of electronic brachytherapy and MMS for the treatment of early-stage non-melanoma skin cancer: a matched pair cohort study. J Contemp Brachytherapy. 2017;4:338–44.
20. Moss WT, Stevens KR, Garcia R. Skin cancer in treatment planning. In: Khan FM, Potish RA, editors. Radiation oncology. Baltimore, MD: Williams & Wilkins; 1998. p. 449–58.
21. Khan FM. The physics of radiation therapy. 4th ed. Lippincott Williams & Wilkins; 2009.
22. https://dotdecimal.com/products/electrons/apertures/.
23. Gunderson L, Tepper J. Clinical radiation oncology. 4th ed. Elsevier; 2016.
24. Morrison WH, Gaden AS, Ang KK. Radiation therapy for non-melanomatous skin carcinoma. Clin Plast Surg. 1997;24:719–29.
25. Guinot JL, et al. GEC-ESTRO ACROP recommendations in skin brachytherapy. Radiother Oncol. 2018;126(3):377–85.
26. Ouhib Z, Kasper M, Perez Calatayud J, Rodriguez S, Bhatnagar A, Pai S, Strasswimmer J. Aspects of dosimetry and clinical practice of skin brachytherapy: The American Brachytherapy Society working group report. Brachytherapy. 2015;14(6):840–58. https://doi.org/10.1016/j.brachy.2015.06.005. Epub 2015 Aug 28.
27. Villalba SR, Perez-Calatayud MJ, Bautista JA, Carmona V, Celada F, Tormo A, García-Martinez T, Richart J, Ortega MS, Silla M, Ballester F, Perez-Calatayud J. Novel simple templates for reproducible positioning of skin applicators in brachytherapy. J Contemp Brachytherapy. 2016;8(4):344–8.
28. Likhacheva AO, Devlin PM, Shirvani SM, Barker CA, Beron P, Bhatnagar A, Doggett SW, Hochman L, Hsu C, Kasper M, Keisch M, Mutyala S, Prestidge B, Villalba SR, Shukla V, Sundararaman S, Kamrava M. Skin surface brachytherapy: a survey of contemporary practice patterns. Brachytherapy. 2017;16(1):223–9.
29. Epstein EH. Basal cell carcinomas: attack of the hedgehog. Nat Rev Cancer. 2008;8:743.
30. Fecher LA, Sharfman WH. Advanced basal cell carcinoma, the hedgehog pathway, and treatment options—role of smoothened inhibitors. Biol Targets Ther. 2015;9:129–40.
31. Lear JT, Migden MR, Lewis KD, Chang ALS, Guminski A, Gutzmer R, Dirix L, Combemale P, Stratigos A, Plummer R, Castro H, Yi T, Mone M, Zhou J, Trefzer U, Kaatz M, Loquai C, Kudchadkar R, Sellami D, Dummer R. Long-term efficacy and safety of sonidegib in patients with locally advanced and metastatic basal cell carcinoma: 30-month analysis of the randomized phase 2 BOLT study. J Eur Acad Dermatol Venereol. 2018;32(3):372. Epub 2017 Nov 6.
32. Basset-Séguin N, Hauschild A, Kunstfeld R, Grob J, Dréno B, Mortier L, Ascierto PA, Licitra L, Dutriaux C, Thomas L, Meyer N, Guillot B, Dummer R, Arenberger P, Fife K, Raimundo A, Dika E, Dimier N, Fittipaldo A, Xynos I, Hansson J. Vismodegib in patients with advanced basal cell carcinoma: primary analysis of STEVIE, an international, open-label trial. Eur J Cancer. 2017;86:334. Epub 2017 Nov 5.

33. Xie P, Lefrançois P. Efficacy, safety, and comparison of sonic hedgehog inhibitors in basal cell carcinomas: a systematic review and meta-analysis. J Am Acad Dermatol. 2018;79(6):1089. Epub 2018 Jul 10.
34. Kim J, Tang JY, Gong R, Kim J, Lee JJ, Clemons KV, Chong CR, Chang KS, Fereshteh M, Gardner D, Reya T, Liu JO, Epstein EH, Stevens DA, Beachy PA. Itraconazole, a commonly used antifungal that inhibits hedgehog pathway activity and cancer growth. Cancer Cell. 2010;17(4):388.
35. Carneiro BA, Watkin WG, Mehta UK, Brockstein BE. Metastatic basal cell carcinoma: complete response to chemotherapy and associated pure red cell aplasia. Cancer Investig. 2006;24(4):396.